Environmental Science & Technology

pubs.acs.org/est

Article

Modeling Novel Aqueous Particle and Cloud Chemistry Processes of Biomass Burning Phenols and Their Potential to Form Secondary Organic Aerosols

Jie Zhang, Manish Shrivastava,* Lan Ma, Wenqing Jiang, Cort Anastasio, Qi Zhang, and Alla Zelenyuk

Cite This: https://doi.org/10.1021/acs.est.3c07762

Read Online

ABSTRACT: Phenols emitted from biomass burning contribute significantly to secondary organic aerosol (SOA) formation through the partitioning of semivolatile products formed from gas-phase chemistry and multiphase chemistry in aerosol liquid water and clouds. The aqueous-phase SOA (aqSOA) formed via hydroxyl radical ($^{\bullet}$OH), singlet molecular oxygen ($^1O_2$*), and triplet excited states of organic compounds (^{3}C*), which oxidize dissolved phenols in the aqueous phase, might play a significant role in the evolution of organic aerosol (OA). However, a quantitative and predictive understanding of aqSOA has been challenging. Here, we develop a stand-alone box model to investigate the formation of SOA from gas-phase $^{\bullet}$OH chemistry and aqSOA formed by the dissolution of phenols followed by their aqueous-phase reactions with $^{\bullet}$OH, $^1O_2$*, and ^{3}C* in cloud droplets and aerosol liquid water. We investigate four phenolic compounds, i.e., phenol, guaiacol, syringol, and guaiacyl acetone (GA), which represent some of the key potential sources of aqSOA from biomass burning in clouds. For the same initial precursor organic gas that dissolves in aerosol/cloud liquid water and subsequently reacts with aqueous phase oxidants, we predict that the aqSOA formation potential (defined as aqSOA formed per unit dissolved organic gas concentration) of these phenols is higher than that of isoprene-epoxydiol (IEPOX), a well-known aqSOA precursor. Cloud droplets can dissolve a broader range of soluble phenols compared to aqueous aerosols, since the liquid water contents of aerosols are orders of magnitude smaller than cloud droplets. Our simulations suggest that highly soluble and reactive multifunctional phenols like GA would predominantly undergo cloud chemistry within cloud layers, while gas-phase chemistry is likely to be more important for less soluble phenols. But in the absence of clouds, the condensation of low-volatility products from gas-phase oxidation followed by their reversible partitioning to organic aerosols dominates SOA formation, while the SOA formed through aqueous aerosol chemistry increases with relative humidity (RH), approaching 40% of the sum of gas and aqueous aerosol chemistry at 95% RH for GA. Our model developments of biomass-burning phenols and their aqueous chemistry can be readily implemented in regional and global atmospheric chemistry models to investigate the aqueous aerosol and cloud chemistry of biomass-burning organic gases in the atmosphere.

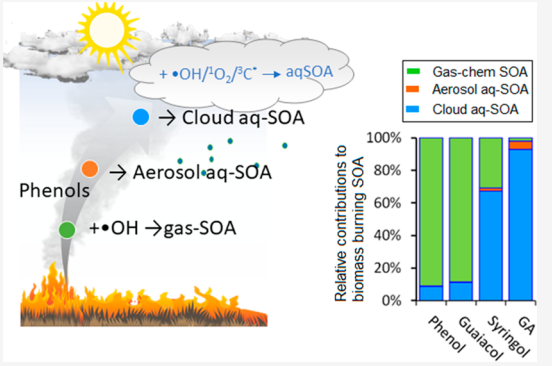

KEYWORDS: *biomass burning, phenols, guaiacyl acetone, aqueous-phase SOA, photooxidants, aerosol liquid water, cloud chemistry*

1. INTRODUCTION

Biomass burning—such as Savanna fires, forest fires, domestic biofuel combustion, and crop residue burning—is a key source of global atmospheric organic aerosols (OA)[1,2] that significantly affects air quality, health, and climate.[3−5] Biomass-burning activities contribute to OA loadings through primary emissions of biomass-burning organic aerosol (BBOA)[6,7] and the formation of secondary organic aerosol (SOA) from reactions of volatile organic compounds (VOCs).[8−11] The contribution from biomass burning to the global SOA budget was estimated at 8−26 Tg yr^{-1} based on laboratory and modeling work.[12] However, models often lack representations of aqueous-phase SOA formation from the reactions of biomass burning organic gases in aerosol and cloud liquid water due to complex aqueous-phase oxidants and chemistry, which are not well understood. In addition, representing these complex chemistry reactions in large scale regional and global Earth System models could be computationally challenging. Ignoring these aqueous chemical processes in regional and global models may underestimate the biomass-burning contributions to the SOA budget and its radiative impact on climate change. In addition to needing reasonable estimation

Received: September 20, 2023
Revised: January 19, 2024
Accepted: January 22, 2024

of emissions,[7] accurately representing the mechanisms of biomass-burning SOA formation in models is also important for analyzing the impacts of biomass burning on air quality and climate.

Phenolic compounds, including phenols and substituted phenols (e.g., methoxyphenols), are important VOCs emitted from biomass burning[7] that can form a great amount of semivolatile products through gas-phase photochemical oxidation reactions.[9,13] The reaction kinetics and SOA formation mass yields from •OH-initiated gas-phase oxidation of phenolic compounds are derived from chamber studies[8,14−17] and can be implemented in regional or global atmospheric chemistry models. In addition, aqueous photochemical oxidation pathways are also significant pathways to form low-volatility SOA in laboratory experiments.[10,18−22] The aqSOA formation is driven by oxidants in the aqueous phase such as hydroxyl radicals (•OH), singlet molecular oxygen ($^1O_2$*), and oxidizing triplet excited states of light-absorbing organic molecules (^{3}C*). The major source of ^{3}C* and $^1O_2$* is brown carbon, i.e., light-absorbing organic molecules, while •OH has multiple sources, including gas-to-aqueous phase partitioning, reactions of iron with peroxides, and direct photolysis of nitrate, nitrite, and organic compounds.[23−28] The aqSOA products, formed from rapid oxidation reactions of phenols, absorb sunlight and are an important source of atmospheric brown carbon.[20,29−32]

Laboratory studies suggest that triplet states and hydroxyl radicals are both important for the formation of aqSOA from phenols: while •OH rate constants are larger than those of ^{3}C*, this is compensated for by higher ^{3}C* concentrations in cloud droplets and, especially, in aerosol particles.[29,31] In cloud droplets, a wide range of phenols can be important aqSOA precursors, including relatively simple phenols that have modest Henry's law constants. However, under the lower liquid water contents of aqueous particles, only highly substituted phenols with higher Henry's law values appear to be significant precursors for aqSOA.[33] Field studies also indicate that aqueous reactions of phenols can be a significant source of new particle mass. For example, Sun et al. reported the detection of phenol aqSOA in both fogwater and aerosol particles collected from California's San Joaquin Valley during the winter season, a period marked by widespread residential wood burning activities.[34] Similarly, Gilardoni et al. identified significant amounts of aqSOA from the reactions of phenols in both fog drops and aqueous aerosol particles in the Po Valley of Italy during winter.[10] More recently, Xiao et al. used winter field measurements from Beijing and laboratory kinetics to estimate an aqSOA formation rate from phenols of 0.42 μg m^{-3} h^{-1}, which accounted for 15% of the total aqSOA observed during the haze pollution.[35] While there is good laboratory and modeling data suggesting that the reactions of phenols in cloud droplets and aerosol particles are significant sources of aqSOA, these processes have not been systematically assessed using modeling techniques and are neglected in most current models.

In this work, we developed a 0-D box model to investigate aqSOA formation in clouds and aqueous aerosols from four individual phenolic compounds (Table S1): phenol, guaiacol (2-methoxyphenol), syringol (2,6-dimethoxyphenol), and guaiacyl acetone (4-hydroxy-3-methoxyphenylacetone, GA). These four compounds among the most abundant phenols in biomass-burning emissions represent fundamental base structures of phenols and encompass a wide range of Henry's law solubilities and reactivities.[31,36,37] None of these compounds absorb sunlight significantly, as illustrated in Figure 2 of Smith et al.[30] The aqueous-phase oxidations of these phenols are driven by reactions with photooxidants such as •OH, ^{3}C*, and $^1O_2$*. All the reactions studied in this work are photochemical in nature, but phenols can also undergo dark reactions with nitrate radicals in the gas and aqueous phases. Given that the reaction rates of nitrate radicals with phenols in the aqueous phase are on the order of 10^8 M^{-1} s^{-1}[38] and estimated nitrate radical concentrations range from 1×10^{-16} to 2.7×10^{-13} M in the dark,[39] these reactions are expected to be less important compared to photochemical aqueous reactions.

Our box model includes semivolatile SOA formed from gas-phase chemistry and its subsequent partitioning to organic aerosol phase[8] and the low-volatility aqSOA formed by kinetic mass transfer of water-soluble organic gases (phenols, IEPOX) to aerosol and cloud liquid water followed by their aqueous phase chemistry based on recent laboratory work within bulk solutions. Our model predicts the multiphase SOA formation potential of biomass-burning organics, providing key insights into the relative role of aqueous and gas-phase chemistry. The aqueous SOA mechanisms developed in our work could be implemented into regional and global air quality models to predict their impacts on SOA formation and radiative forcing.

2. METHODS

2.1. Phenolic SOA Formation from Gas-Phase Chemistry. SOA formation from •OH-initiated gas-phase chemistry was described in the dry chamber experiments of Yee et al.[8] The mass yields of SOA products are described using the volatility basis set (VBS) approach (Section S1). The reaction rate coefficients (k_{OH}) measured in the previous studies and the derived volatility basis set (VBS) parameters for SOA products are listed in Table S2. SOA products from gas-phase oxidation reactions with guaiacol and syringol are semivolatile with saturation mass concentrations (C^*) of 10−100 μg m^{-3}. Figure S1 shows the dependence of SOA yields on OA concentration (C_{OA}), which were determined by fitting a 4-product VBS to the high NO_x experiments of Yee et al.[8] As there are no reported yields for GA-SOA from gas-phase chemistry, we model GA-SOA using the literature k_{OH} and the SOA yield reported for guaiacol. Both the high and low NO_x experiments of Yee et al.[8] indicated similar yields for guaiacol; therefore, GA and guaiacol yields used in this work are expected to apply over high and low NO_x regimes.

2.2. Air−Water Partitioning of Phenolic Compounds. The equilibrium partitioning between the gas and aqueous phases is described by the Henry's law constant (H^*), which is defined as the ratio of aqueous concentration in mol L^{-1}-solution (M) to the gas-phase partial pressure in atm. Henry's law constants under standard temperature (298 K) for the four phenols were reported in the experimental studies.[36,40,41] These values are within the possible range reported by the previous studies according to Sander's most recent literature review (Table S1).[42] The temperature-dependent Henry's law constant (H_T^*) is expressed using the reformatted Van't Hoff form, as eq 1:

$$\ln(H_T^*) - \ln(H_{298K}^*) = -\frac{\Delta H_{sol}}{R}\left(\frac{1}{T} - \frac{1}{298}\right) \quad (1)$$

https://doi.org/10.1021/acs.est.3c07762
Environ. Sci. Technol. XXXX, XXX, XXX−XXX

where H^*_{298K} is the Henry's law constant at 298 K (M atm^{-1}); ΔH_{sol} is the enthalpy of solvation (J mol^{-1}); R is the ideal gas constant (J mol^{-1} K^{-1}); and T is the air temperature (K). Based on the measurements of McFall et al.,[36] Henry's law constants increase by factors of 5−8 when the temperature is decreased from 298 to 278 K, resulting in increasing partitioning of phenols into aqueous particles and cloud droplets as temperature decreases in the atmosphere.

2.3. Aqueous-Phase Reaction Kinetics and aqSOA Mass Yield of Phenols. We consider aqueous-phase reactions of phenols with three oxidants, $^{\bullet}$OH, $^1O_2$*, and ^{3}C*, in aerosol water and cloud droplets. Reaction rate constants are from bulk-solution measurements in the laboratory, as shown in Table S3.[29,31,37,43] While ^{3}C* is a complex mixture that depends on the dissolved organic and brown carbon content of particles and cloud droplets, bulk solution measurements in the laboratory simulate its average reactivity with the triplet excited state of 3,4-dimethoxybenzaldehyde (DMB).[30,31] Past kinetic experiments for phenols with ^{3}C* were performed at pH 2 and 5 to characterize the reactivity with the protonated and neutral triplet states of DMB, respectively. The mole fractions of neutral triplet (α_T) and protonated triplet (α_{HT}) are estimated using eq 2:

$$\alpha_T = \frac{1}{1 + \frac{[H^+]}{K_{a,DMB}}}; \quad \alpha_{HT} = 1 - \alpha_T \tag{2}$$

where $[H^+]$ is the concentration of H^+ in the solution (M) and $K_{a,DMB}$ is the equilibrium constant of DMB protonation, which has a pK_a of 3.3 ± 0.2.[29,44] Therefore, the second-order reaction rate constant of phenols with ^{3}C* ($k_{ArOH,^3C*}$) at a given pH is a mole-fraction-weighted average of the constants at pH 2 ($k_{ArOH+HT}$) and 5 (k_{ArOH+T}):

$$k_{ArOH,^3C*} = \alpha_{HT} k_{ArOH+HT} + \alpha_T k_{ArOH+T} \tag{3}$$

Reaction rate constants for phenols with the protonated triplet state of DMB are faster than those with the neutral triplet state by a factor of 26 for phenol and factors of 1.2−1.9 for guaiacol, syringol, and GA (Table S3). In contrast, the reaction rate constants for $^{\bullet}$OH ($k_{ArOH,OH}$) at pH 5 are higher than those at pH 2. Since the detailed pH dependence of $k_{ArOH,OH}$ has not been reported, we applied the $k_{ArOH,OH}$ measured at pH 2 for model conditions when pH < 3.5 and used the measured rate constant at pH 5 for model conditions of pH ≥ 3.5. The second-order reaction rate constants for phenols with $^1O_2$* ($k_{ArOH,^1O_2^*}$) were measured under high pH (pH = 6−12),[43] which is higher than the typical pH of atmospheric aerosols or cloud droplets.[45−48] However, $k_{ArOH,^1O_2^*}$ is generally constant for pH less than 8,[43] so we use rate constants at pH 6 since this likely represents the kinetics under more acidic conditions.

The mass yield of phenolic aqSOA formed with $^{\bullet}$OH and ^{3}C*, i.e., the mass of SOA formed per mass of phenolic compound reacted, was determined in real-time by high-resolution time-of-flight aerosol mass spectroscopy (HR-ToF-AMS).[29] AqSOA mass yields were determined in reaction solutions with a pH of 5 because the acidic solutions (pH 2) were highly hygroscopic due to the large amount of sulfuric acid, making it challenging to quantify SOA mass using AMS.[29−31,37] Mass yields were high, 0.8−1.4, for phenols reacting with $^{\bullet}$OH and ^{3}C* due to efficient oligomerization and incorporation of oxygen into the products.[22,32,34] There are no yields reported for aqSOA from phenols oxidized by $^1O_2$*, so we assumed a value of 1.0.

Using our box model, we predict concentrations of $^1O_2$ and ^{3}C* in cloud droplets and aerosol liquid water (ALW) based on their relations with dissolved organic carbon (DOC) derived from measurements in dilute extracts of ambient $PM_{2.5}$ as shown in Figure 3a. The parametrization of oxidant concentrations in this work is based on measurements of ambient PM under atmospheric photochemical conditions normalized to midday winter solstice sunlight in Davis, California (corresponding to a solar zenith angle of 62°) and are described in Supplementary Section S3.

2.4. Stand-Alone Box Model Development for Phenolic SOA. We developed a stand-alone box model to simulate gas-phase reactions with $^{\bullet}$OH, gas-particle partitioning of semivolatile SOA products, uptake of water-soluble organic gases, and aqSOA formation in cloud droplets and ALW. Organic gases such as phenols and IEPOX can partition into both cloud droplets and aerosols; however, in our box model we do not consider interaction between aerosols and clouds such as aerosol activation and cloud droplet evaporation. The objective of our work was to develop a conceptual understanding of aerosol and cloud chemistry within a simple box model. The formation of SOA via gas-phase reactions (i.e., gas-SOA) from $^{\bullet}$OH-initiated reaction of phenols and the gas-particle partitioning of reaction products follow experiments in Yee et al.,[8] as discussed in Section S1.

AqSOA formation in cloud droplets is simulated using the reduced version of the Gas−Aerosol Model for Mechanism Analysis (SimpleGAMMA),[49] which has been successfully applied to simulate aqSOA formation from important water-soluble trace gases, e.g., isoprene-epoxydiol (IEPOX), in box and regional atmospheric chemistry models.[50−53] Compared to cloud droplets, the ALW concentration in aerosols is several orders of magnitude lower, and we use the irreversible reactive surface uptake approach to simulate the kinetics of aqSOA formation. This approach has been widely used for modeling aerosol heterogeneous reactions of N_2O_5, IEPOX, glyoxal, and methylglyoxal.[54−58] These two approaches, i.e., simpleGAMMA and irreversible reactive surface uptake for simulating aqueous chemistry in cloud and aerosol liquid water, respectively, are described in Supplementary Section S4.

2.5. Model Setup. With our idealized box model simulations, we simulate two cases: (1) the cloud case (clean and polluted), in the proximity of shallow liquid clouds where SOA is formed by chemistry in the gas phase, in aqueous aerosol particles, and in cloud droplets, and (2) the surface case, a cloud-free, near-surface scenario where SOA is formed by chemistry in the gas phase and in aqueous aerosol particles with relative humidity varying in the range of 50−95%. We assume an initial 1 ppb of an individual phenolic compound (i.e., phenol, guaiacol, syringol, and GA) and a uniform size distribution of cloud droplets and aerosols. To investigate the sensitivity of SOA formation to meteorological conditions and aerosol/cloud properties, we conduct simulations with varying environmental conditions, e.g., RH, number concentration of aerosols and cloud droplets, liquid water content (LWC), and OA loadings.

In the cloud case, there exist both activated cloud droplets and unactivated aqueous aerosol particles, which can both dissolve water-soluble phenols and form aqSOA via photo-oxidation reactions. Near the clouds, we assume that the temperature is approximately 5 °C (278 K) and that the RH is

https://doi.org/10.1021/acs.est.3c07762
Environ. Sci. Technol. XXXX, XXX, XXX−XXX

nearly saturated (98%). The selected temperature of 5 °C represents winter humid conditions in areas where residential wood burning for heating is prevalent and BBOA dominates OA composition, such as the Central Valley of California and some European cities.[59,60] Lower temperatures correspond to winter foggy conditions in areas with anthropogenic BB emissions, and higher temperatures can occur in clouds impacted by wildfires. Under clean conditions, the aerosol number concentration is assumed as 10^3 cm^{-3}, with submicrometer particle mass concentrations of 6.0 $\mu g\ m^{-3}$ NH_4HSO_4, 1.0 $\mu g\ m^{-3}$ BBOA, and 1.0 $\mu g\ m^{-3}$ OOA, which are reasonable assumptions as a background rural condition.[52,61,62] For these assumed background inorganic aerosol mass concentrations and meteorological conditions, we calculate an aerosol pH of 0.48 using the online Extended AIM Aerosol Thermodynamics Model[63] (E-AIM, available at http://www.aim.env.uea.ac.uk/aim/aim.php). The ALW includes water associated with inorganic ions (ALW_{inorg}) of 8.9×10^{-5} g m^{-3} calculated by E-AIM and the water associated with the organics (ALW_{org}) of 8.2×10^{-6} g m^{-3} that is estimated by Kappa-Köhler theory. Only ALW_{inorg} is associated with the uptake of phenols in the aerosols, while ALW_{org} participates in determining the particle wet diameter and DOC molarity, as shown in Table S5. Note that the dry diameters of particles are at least a factor of 2 smaller than the wet diameters determined in Table S5. Under polluted conditions, the assumed aerosol number concentration is 10^4 cm^{-3}, and the BBOA and OOA mass concentrations are both increased to 10 $\mu g\ m^{-3}$, which represents the typical conditions in polluted urban areas.[62,64,65] Meteorological conditions and inorganic aerosols are assumed to be the same as those in the clean case. Clean and polluted aerosols are assumed to change cloud droplet concentrations and cloud liquid water, as described below.

Our clean cloud case assumes a cloud droplet number concentration of 10 cm^{-3} and an LWC of 0.1 g m^{-3}, which results in the large drop diameter of 26.7 μm, assuming uniform size distribution. Under polluted conditions, the cloud droplet diameter is 8.6 μm, the number concentration is 3000 cm^{-3}, and the LWC is 1.0 g m^{-3}. The given mass concentrations of BBOA and OOA in the cloudy air translate to much lower concentrations per unit liquid water within cloud droplets compared to in unactivated aerosol particles, since clouds have much more liquid water compared to aerosols. As shown in Figure 3a, photooxidant concentrations are sensitive to [DOC] in clouds; therefore, aqSOA formation could be faster in air masses containing biomass-burning plumes. To examine this case of high BBOA, we conduct a sensitivity simulation increasing the BBOA concentration to 100 $\mu g\ m^{-3}$, resulting in a cloud [DOC] of 2.3×10^{-3} mol C L^{-1},as shown in Table S5. The cloud case simulations were run for 20 min, which is the typical lifetime of shallow liquid clouds.

In the surface case, the ALW in the aerosols is the only medium for aqueous-phase photooxidation reactions and aqSOA formation. The aerosol number and mass concentrations are assumed to be similar to the polluted conditions in the cloud case, as shown in Table S6. AqSOA formation is investigated at 5 °C (278 K) and moderate to high humidity (50−95% RH). The ALW_{inorg} calculated by E-AIM is 52−62% of the total ALW associated with both inorganic ions and organics in the aerosols with varying RH. The [DOC] is calculated with total ALW by assuming that 37% of BBOA and 49% of OOA is water-soluble.[66,67] As shown in Figure 3a, when [DOC] is higher than 0.1 mol C L^{-1}, the steady-state [$^3C^*$] does not change and [$^1O_2^*$] decreases; therefore, highly concentrated [DOC] is not likely to overestimate aqSOA formation in the particles. The surface case was run for longer simulation times of 2 h compared to the cloud case (20 min).

3. RESULTS AND DISCUSSIONS

Our newly developed box model examines aqSOA formation from phenols in clouds and aerosols based on the most recent laboratory data. Our simulations cover varying environmental parameters to show the contributions of SOA formation from phenolic compounds in both gas and aqueous phases under certain conditions, as discussed below. This provides unique insight into the novel aqueous chemistry of phenols in clouds and aerosol water and their potential to form atmospheric SOA.

3.1. AqSOA Formation in the Cloud Case. In the cloud case, phenolic SOA formation occurs through gas-phase $^{\bullet}OH$-initiated photooxidation, reactive uptake of phenols in the aerosol particles, and the dissolution and reactions of dissolved phenols within the cloud droplets. As shown in Figure S2, for our assumed 1 ppb initial phenol concentration, gas-phase chemistry is important for phenol, syringol, and guaiacol, producing 0.05−0.2 $\mu g\ m^{-3}$ gas-SOA within the cloud layer after 20 min. However, for GA, the gas-phase chemistry contribution is negligible since GA rapidly dissolves within the large cloud liquid water and undergoes cloud chemistry. Thus, our simulations suggest that highly soluble and reactive multifunctional phenols like GA would predominantly undergo cloud chemistry within cloud layers, which agrees with a previous study that suggested cloud processing of substituted aromatic compounds to be an effective formation pathway of aqSOA.[68] In addition, our predicted lifetime of phenols in clouds due to aqueous oxidation by $^{\bullet}OH$ is ∼6 h, similar to the ∼9 h estimated lifetime of phenols in clouds estimated by Hoffmann et al.[68] Gas-phase chemistry followed by partitioning to the organic aerosol phase is likely to be more important for less soluble phenols compared to their partitioning to the aqueous phase and subsequent aqSOA formation. Under polluted conditions, the concentration of gas-SOA is slightly higher than that of gas-SOA formed under clean conditions due to the higher OA loadings, which allows for higher semivolatile SOA product partitioning. Compared to cloud-phase aqSOA, aerosol-phase aqSOA is negligible within cloudy layers because the LWC in aerosols is several orders of magnitude lower than that in the cloud droplets. Under polluted conditions, the cloud droplets also have a higher LWC and smaller sizes compared to clean conditions. The gas-to-particle mass transport is faster for smaller compared to larger droplets due to gas-phase diffusion, and the final equilibrium droplet concentration increases with the cloud liquid water content. Therefore, in polluted conditions characterized by smaller cloud droplets and higher cloud LWC compared to clean conditions, the soluble gases dissolve more quickly and increase the level of aqSOA formation compared to clean conditions.

Compared with the simple phenols (i.e., phenol, guaiacol, and syringol), which have Henry's law constants H^*_{298K} of $(3.4-25) \times 10^3$ M atm^{-1} at 5 °C, the more highly substituted phenol GA is highly soluble with $H^*_{298K} = 9.1 \times 10^6$ M atm^{-1}, which is comparable with IEPOX. IEPOX, an important product from isoprene oxidation under low-NOx conditions, is a key source of aqSOA in atmospheric particles.[69,70] In

https://doi.org/10.1021/acs.est.3c07762
Environ. Sci. Technol. XXXX, XXX, XXX−XXX

addition, IEPOX-SOA has been observed in cloud droplet residuals[71] and modeled in clouds through acid-catalyzed reactions[72−74] and the •OH-mediated oxidation pathway that does not depend on acidity.[75] Figure 1 compares the cloud chemistry of IEPOX and GA that results in SOA formation, and for this comparison, we only simulate cloud chemistry turning off the gas-phase and aqueous aerosol chemistry within our box model for both IEPOX and GA. Figure 1a shows that with an initial mixing ratio of 1 ppb and only considering cloud-phase formation of aqSOA (as described in Figure 1d), both IEPOX (MW = 118 g mol^{-1}) and GA (MW = 182 g mol^{-1}) almost entirely dissolve in the cloud droplets within ∼7 min under clean conditions and almost instantly under polluted conditions. Within the aqueous phase, the acid catalyzed ring opening of IEPOX followed by nucleophilic addition results in the formation of IEPOX-SOA that has two major components: 2-methyltetrols when water is the nucleophile and organosulfates when sulfate is the nucleophile. In addition to the acid catalyzed pathway, we also include IEPOX-SOA formation from aqueous-phase •OH oxidation within cloud droplets using temperature-dependent oxidation kinetics of dissolved IEPOX from Otto et al.[75] and assuming the aqSOA mass yield of 1.0 as an upper bound to IEPOX-SOA formation resulting from this pathway. The simulated IEPOX pseudo-1st-order reaction rate constant is calculated as 5.0×10^{-6} s^{-1} for acid-catalyzed reactions (with pH 4) and 5.4×10^{-6} s^{-1} for •OH mediated reaction in cloud droplets. About half of our simulated IEPOX-SOA is formed through the OH oxidation pathway (acidity independent), and the other half is mainly comprised of 2-methyltetrols since the concentration of SO_4^{2-} is low within clouds, suppressing the formation of organosulfates. In comparison to IEPOX-SOA kinetics, for the assumed conditions in Table S5, the calculated pseudo-1st-order reaction rate constant for GA of 1.8×10^{-4} s^{-1} is ∼2 orders of magnitude greater within the cloud droplets. Therefore, the simulated aqSOA formed after 20 min from GA oxidation is an order of magnitude higher than that from IEPOX due to the much faster reaction rate of GA within clouds (Figure 1b). Note that although the acid-catalyzed formation of IEPOX-SOA in aqueous aerosols strongly depends on particle acidity, the acidity is lower in cloud droplets due to its buffering from the large cloud liquid water content.

The other three phenolic compounds have comparable photooxidation reaction rate constants as GA, with overall pseudo-1st-order reaction rate constants (as described in eq S4.3) of 1.1×10^{-4}, 2.9×10^{-4}, and 4.3×10^{-4} s^{-1}, for phenol, guaiacol, and syringol, respectively. As shown in Figure 1c, after 20 min under clean conditions, the simulated amounts of aqSOA from phenol and guaiacol (0.005 and 0.018 μg m^{-3}, respectively) are much lower than those of IEPOX-SOA (0.06 μg m^{-3}) because of their low Henry's law constants, while the amounts of aqSOA from syringol and GA (0.16 and 1.23 μg

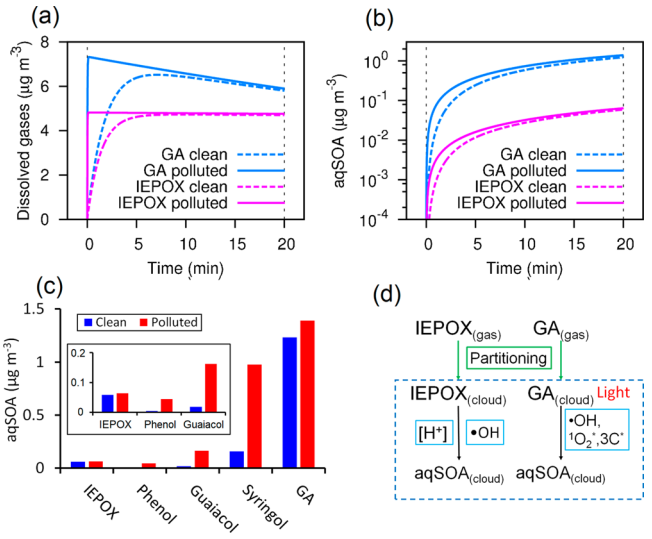

Figure 1. Box model simulated time evolution within clouds of (a) dissolved IEPOX and GA gases and (b) aqSOA formed in cloud droplets under clean and polluted cloud conditions with an initial gas-phase mixing ratio of 1 ppb; (c) aqSOA formed from dissolved IEPOX and phenols in cloud droplets at the end of 20 min of simulation; and (d) schematic of cloud-phase aqSOA mechanism implemented in the box model. Note: 48% of IEPOX-SOA is formed from the •OH-mediated oxidation pathway within clouds, while the remaining 52% is through acid-catalyzed reactions.

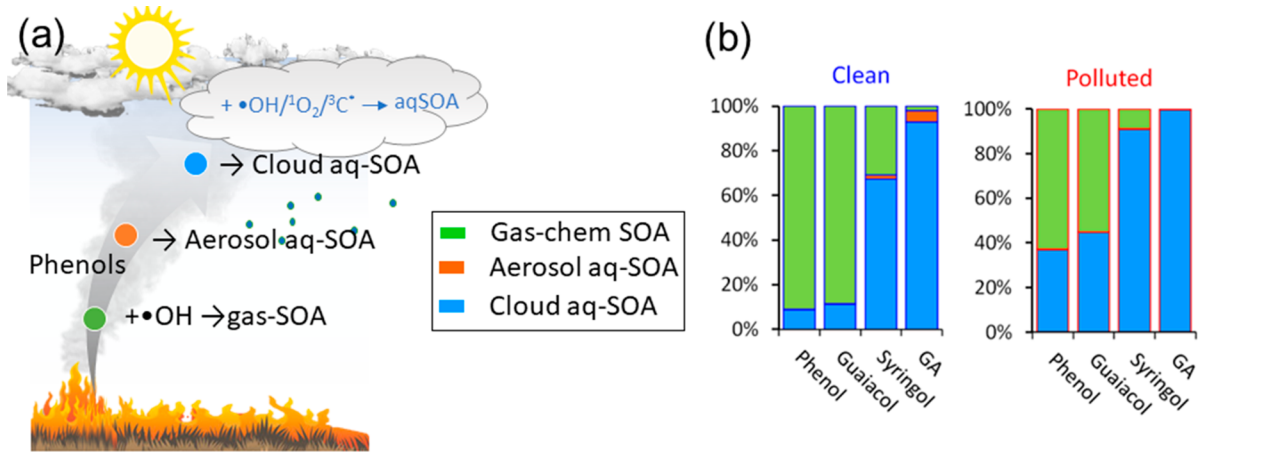

Figure 2. (a) Schematic depicting that soluble phenols emitted from biomass burning undergo gas-phase oxidation followed by reversible partitioning into the organic phase (Gas-chem SOA), dissolving in aerosol and cloud liquid water, and reacting with aqueous-phase oxidants to form aqSOA in aerosols (Aerosol aq-SOA) and clouds (Cloud aq-SOA). (b) Relative contributions to biomass burning SOA formation from gas-phase chemistry (green), aqueous aerosol chemistry (orange), and cloud chemistry (blue) under clean and polluted conditions.

https://doi.org/10.1021/acs.est.3c07762
Environ. Sci. Technol. XXXX, XXX, XXX−XXX

m^{-3}, respectively) are much higher. Under the higher LWC condition of the polluted case, higher fractions of the phenols are dissolved in the cloud droplets (Figure S2), resulting in faster rates of aqSOA production.

To investigate the relative contributions of gas-phase and aqueous-phase reactions to the total SOA formation in the cloud case, we next enabled all three SOA formation processes competing for a given phenolic gas concentration: (1) gas-chem SOA, (2) aqSOA in aerosols, and (3) aqSOA in clouds, as shown in Figure 2a. Figure 2b shows that in the cloud case, aqSOA formation in aerosols contributes less than 5% to total SOA under clean conditions and is negligible under polluted conditions. Under clean conditions (Figure 2b), aqSOA formation in cloud droplets contributes ~10% of total SOA for phenol and guaiacol, 67% for syringol, and 93% for GA. AqSOA formation in cloud droplets becomes even more important under polluted conditions with contributions to total SOA of 37% for phenol, 45% for guaiacol, 91% for syringol, and 100% for GA. In the atmosphere, the lifetime of cloud droplets ranges from minutes to a few hours, which are smaller than the lifetime of submicrometer aerosols (~days to a week). But in cloud-affected regions of the atmosphere, as cloud droplets go through several cycles of evaporation and reactivation due to mixing/entrainment of ambient air parcels in clouds, cloud processing of aerosols could cause substantial aqSOA formation through both cloud and aerosol aqueous chemistry. These results show that the phenolic aqSOA formation in cloud droplets is a significant source of SOA and could contribute more than traditional semivolatile SOA formation pathways, especially in polluted cases with high cloud LWC.

In contrast to Figure 2 above, where clouds and aerosols compete for available phenolic gases, there are many instances in which clouds and aerosols exist separately and do not compete for gas-phase phenols. In the absence of this competition, we found that aqSOA concentrations in cloud-water (per unit dry air volume) are higher than in aerosol water due to more dissolved gases in larger cloud volumes. However, the aqSOA formation potential (i.e., the amount of aqSOA formed per unit of dissolved phenols) is ~2 orders of magnitude higher in aerosol water compared to cloudwater (Figure S3) due to much higher oxidant concentrations in aerosol water (shown as CA-1 in Figure 3a).

$^{\bullet}OH$ and $^{3}C^{*}$ are the dominant contributors to the formation of aqSOA from phenols in the cloud droplets. Although the steady-state concentration of $^{1}O_2^{*}$ is higher than that of $^{3}C^{*}$ and, especially, $^{\bullet}OH$, the $^{1}O_2^{*}$-mediated aqSOA formation rate is several orders of magnitude lower due to low reaction rate constants (Figure S4). Both $[^{1}O_2^{*}]$ and $[^{3}C^{*}]$ are sensitive to [DOC] in cloud droplets, which is estimated by the dissolved BBOA and OOA concentrations. We also simulated a polluted (high LWC) cloud case (CC-3 in Table S5) with a much higher BBOA concentration (100 $\mu g\ m^{-3}$), representative of a biomass-burning plume. Compared to the 10 $\mu g\ m^{-3}$ low BBOA-high LWC) cloud case (CC-2), $[^{1}O_2^{*}]$ and $[^{3}C^{*}]$ simulated in CC3 (high BBOA of 100 $\mu g\ m^{-3}$ and high LWC cloud case) increase by a factor of 4–5 (as shown by the first two points of each line in Figure 3a). Therefore, our simulations predict that increasing BBOA from 10 to 100 $\mu g\ m^{-3}$ increases aqSOA formation by a factor of 2–3 within clouds with high LWC (Figure 3b) due to increased concentrations of $^{1}O_2^{*}$ and $^{3}C^{*}$, as shown in Figure 3a. While we assumed a temperature of 5 °C for all prior

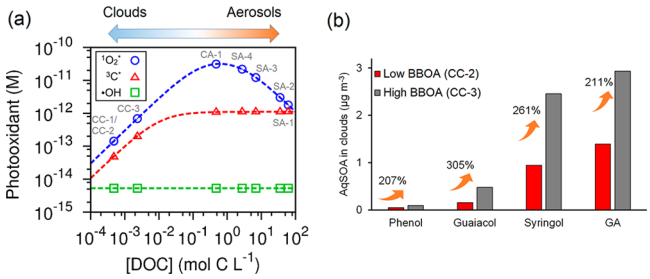

Figure 3. (a) Box model simulated photooxidant concentrations as functions of [DOC] in cloud droplets and aerosol liquid water. [$^{\bullet}OH$] is assumed as a constant of 5.3×10^{-15} M, as described in the text. $[^{1}O_2^{*}]$ is calculated using eq S3.13 with the parameters in Table S4. $[^{3}C^{*}]$ is calculated using eq S3.6 and parameters in Table S3. The points show the concentrations of photooxidants in the simulations of cloudy-layer and near-surface cases (as in Table S4, CC-1: cloud droplets in the clean cloud case; CC-2: cloud droplets in the polluted cloud case with low BBOA; CC-3: cloud droplets in the polluted cloud case with high BBOA; CA-1: aerosols within cloudy layers in the clean cloud case; SA-1: aerosols in the surface case with 50% RH; SA-3: aerosols in the surface case with 70% RH; SA-4: aerosols in the surface case with 90% RH; SA-4: aerosols in the surface case with 95% RH). (b) Simulations showing the enhanced aqSOA formation through cloud chemistry of dissolved phenols when the primary BBOA concentrations increase from 10 to 100 $\mu g\ m^{-3}$. For each case, the initial mixing ratio of the phenolic compound was 1 ppb.

calculations, as discussed earlier, we also investigated the effects of cloud temperature through sensitivity simulations for the polluted cloud case with high BBOA (100 $\mu g\ m^{-3}$) as discussed in Supplemental section S6 (Figure S6). At ~25 °C, our simulations show that aqSOA formation is reduced by 60–80% compared to 5 °C for less-soluble gases (phenol and guaiacol). However, for highly soluble phenols such as GA, the aqSOA concentration is less sensitive to temperature.

3.2. AqSOA Formation in the Surface Aerosol Case.

We next consider a case with only particle water (i.e., in the absence of a cloud), where aqSOA can form in ALW. As shown in Table S6, the liquid water content of the aerosol increases by an order of magnitude from 4.4×10^{-6} g m^{-3} at 50% RH to 6.6×10^{-5} g m^{-3} at 95% RH. The cloud-free, surface case simulations discussed above are run under elevated (50% RH) to high RH (95%RH) and a temperature of 278 K to reproduce the winter meteorological conditions in California's Central Valley.

The concentrations of gas-SOA and aqSOA formed after 2 h of simulations are shown in Table S8. The concentration of gas-SOA formed by OH oxidation of 1 ppb phenol is 0.45–1.53 $\mu g\ m^{-3}$, which is the dominant contributor to the total SOA in the aerosols. The aqSOA formation in the aerosol particles greatly increases as RH increases; e.g., the concentration of aqSOA at 95% RH is higher than that at 50% by a factor of ~6 (Figure 4a,b). Aqueous aerosol concentrations of oxidants $^{\bullet}OH$ and $^{3}C^{*}$ are mostly constant between 50 and 95% RH as shown in Figure 3a (SA-1:50% RH, SA-4:95% RH, as in Table S6), however, simulated concentration of $^{1}O_2^{*}$ increases by ~1–2 orders of magnitude as RH increases from 50% to 95%. In aerosol water, the [DOC] is several orders of magnitude higher than in clouds (Table S6 versus Table S5) and simulated $[^{3}C^{*}]$ is much higher than [$^{\bullet}OH$], which is roughly independent of [DOC] as discussed in Ma et al.[76] Our simulations show that the $^{3}C^{*}$ photooxidation pathway is the dominant contributor to aqSOA

https://doi.org/10.1021/acs.est.3c07762
Environ. Sci. Technol. XXXX, XXX, XXX−XXX

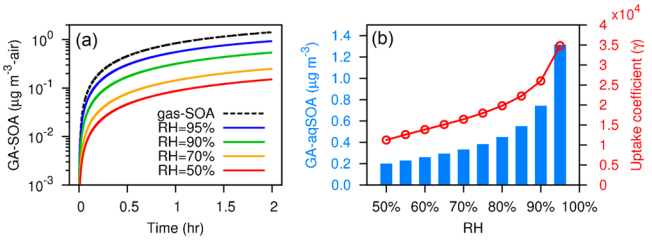

Figure 4. (a) Simulated time evolution of gas-SOA and aqSOA in aerosol liquid water near the surface (in the absence of clouds) by the oxidation of an initial 1 ppb concentration of GA under an RH of 50−95%. (b) Concentration of GA-aqSOA at 2 h (blue bars) and uptake coefficient of GA (red circles and the connecting line) under RH of 50−95%.

in aerosol water and is several orders of magnitude higher than aqSOA formed through the other two oxidants (Figure S7). Only the aqSOA formed from highly soluble GA at high RH (0.93 μg m^{-3} at 95% RH) is comparable with the gas-chem SOA (1.5 μg m^{-3}), as shown in Figure 4a, while concentrations of aqSOA formed from the other less-soluble phenols are much lower than those of GA in aerosols. The simulated reactive uptake coefficient (γ) of GA also increases with RH, increasing from 1.1×10^{-4} at 50% RH to 3.5×10^{-4} at 95% (see Figure 4b). This suggests that GA could be an important source of aqSOA in aerosols, especially at high RH approaching fog conditions. Other highly substituted phenols with high Henry's law constants are likely similarly important, as discussed later.[36]

Our simulations indicate that compared to clouds, aqSOA formation in aerosol water is negligible due to a smaller liquid water volume in aerosol compared to clouds for dissolution of soluble organic gases. But the average lifetime of aerosols in the atmosphere is on the order of several days, while the lifetime of a cloud droplet is on the order of several minutes to a few hours. Our box model does not consider the impacts of differing lifetimes of aerosols versus cloud droplets on aqSOA formation in the real atmosphere, which can be better accounted for by detailed regional model simulations. However, our idealized simulations show that within cloudy layers cloud chemistry will dominate aqSOA formation in the atmosphere as clouds take up most of the soluble phenols due to their large liquid water content and will outcompete interstitial, unactivated aerosols for phenols. Near the surface, the contribution of cloud chemistry to phenols in aerosols might still be significant as cloud chemistry within clouds at the top of the boundary layer and subsequent evaporation of cloud droplets add to aerosol loadings, and these aerosols are mixed down from cloud layers to the surface with boundary layer mixing. In situ aqSOA formation near the surface is mostly determined by chemistry in aerosol liquid water in the absence of fog/clouds. Therefore, detailed regional model simulations are needed to account for different aqSOA pathways occurring over different spatial and temporal scales in cloud droplets and aerosols in the atmosphere.

In addition to the simple phenols (i.e., phenol, guaiacol, and syringol), McFall et al. measured and compiled Henry's law constants for more complex biomass-burning phenols.[36] These compounds span a large range of Henry's law constants varying across 6 orders of magnitude. In addition to GA, other highly substituted phenols like vanillin, syringaldehyde, and syringyl acetone, observed in biomass burning field studies, could be significant sources of aqSOA as discussed in Supplementary Section S8, but they are not considered in models. Ignoring aqSOA formed by these soluble phenols could lead to significant underpredictions of SOA formation from aqueous and cloud chemistry in regions influenced by biomass burning.

Maximizing accuracy and computational efficiency is critical for implementation of aqueous SOA formation modules in three-dimensional chemical transport models. The modeling time step of chemical processes determines the computational cost. Smaller time steps are needed for accurate simulations of rapid dissolution and chemistry processes, but these small time steps significantly increase the computational cost of simulations. However, larger time steps could lead to biases in simulated aqSOA, although they reduce the computational expense. Therefore, finding the appropriate time step for the aqSOA formation processes is necessary to maximize the accuracy and computational efficiency in regional or global modeling studies. In Supporting Information, Section S9, we show that the reactive surface uptake approach is an integral approach, which is not as sensitive to time steps as the simpleGamma approach. Therefore, the reactive surface uptake approach is amenable to simulate aerosol-phase aqSOA formation from phenols, and the typical regional model time step of ~ minutes can be used for aerosol aqSOA simulations. However, the simpleGamma approach, which treats dissolution of phenols and their subsequent reaction in cloudwater and thus separates the processes of dissolution and chemical reaction in cloud water, is needed for cloud chemistry of phenols and necessitates a smaller time step less than 0.1 s.

3.3. Discussion. We simulated multiphase chemistry that includes dissolution of water-soluble organic gases emitted by biomass burning within aerosol and cloud liquid water followed by their aqueous-phase reactions to form aqueous SOA. Within cloud layers, we found that highly soluble and reactive multifunctional phenols like GA are almost entirely dissolved and react in cloudwater causing SOA formation that greatly exceeds the gas-phase chemistry of GA. Even near the surface in the absence of clouds, these highly soluble phenols form significant amounts of SOA in aqueous aerosols since they can be easily dissolved in aerosol liquid water and are available for aqueous aerosol chemistry. However, for less soluble phenols, we find that gas-phase chemistry is likely to be more important than cloud chemistry at cloud levels and near the surface even at high RH. However, highly soluble multifunctional phenolic compounds form significant amounts of aqSOA in aqueous aerosols since they can be easily dissolved in aerosol liquid water and are available for aqueous aerosol chemistry.

In addition to the directly emitted soluble VOCs from biomass burning, highly soluble oxidation products derived from the multigenerational gas-phase oxidation of biomass burning VOCs including phenols, furans, and heterocyclic aromatics could easily dissolve in the aqueous phase and form aqSOA. The aqSOA formation potential of these multigeneration oxidation products can then be evaluated on regional and global scales using detailed regional models such as WRF-Chem and global climate models, respectively. The key would be to identify focused field experiments and advanced instruments with specific chemical measurements in the gas phase and aerosol and cloud liquid water that could help identify the potential role of aqSOA formation to evaluate aqSOA predicted by regional and global models.

Over the past decade, aqueous chemistry from biogenic isoprene forming IEPOX-SOA has been shown to be important in the atmosphere, but aqueous SOA budgets of

https://doi.org/10.1021/acs.est.3c07762
Environ. Sci. Technol. XXXX, XXX, XXX−XXX

biomass burning organic gases are not well understood. For the same initial gas-phase precursor concentrations, our simulations show that although both GA and IEPOX gases are highly water-soluble, mass concentration of GA-SOA formed in cloud droplets is 2 orders of magnitude higher than IEPOX-SOA due to much faster aqueous-phase reaction rates of GA compared to IEPOX. The formation of aqSOA from highly soluble multifunctional phenols is not included in current regional or global atmospheric chemistry models, which could underestimate the biomass-burning contributions to SOA budgets. As wildfires continue to increase in frequency and severity and are transported thousands of miles, the reactions of soluble organic gases that form aqueous-phase SOA in aerosols and clouds might be important.

■ ASSOCIATED CONTENT

Supporting Information

The Supporting Information is available free of charge at https://pubs.acs.org/doi/10.1021/acs.est.3c07762.

Additional information on phenol properties and SOA formation from gas-phase chemistry (Section S1), SOA formation from aqueous-phase chemistry (Section S2), estimation of aqueous photooxidant concentrations (Section S3), model process of aqSOA formation in cloud droplets and aerosol water (Section S4), model simulation conditions (Section S5), simulation results for the cloud case (Section S6), simulation results for aerosol case (Section S7), aerosol-phase aqSOA formation sensitivity to the Henry's Law constant of phenols (Section S8), sensitivity of computational time step (Section S9), and references (PDF)

■ AUTHOR INFORMATION

Corresponding Author

Manish Shrivastava − *Pacific Northwest National Laboratory, Richland, Washington 99352, United States;* orcid.org/0000-0002-9053-2400; Email: manishkumar.shrivastava@pnnl.gov

Authors

Jie Zhang − *Pacific Northwest National Laboratory, Richland, Washington 99352, United States*

Lan Ma − *Department of Land, Air and Water Resources, University of California, Davis, California 95616-8627, United States; Agricultural and Environmental Chemistry Graduate Group, University of California, Davis, California 95616-5270, United States;* Present Address: SGS-CSTC Standards Technical Services Co. Ltd., Hangzhou Branch, Hangzhou, Zhejiang Province 310052, China; orcid.org/0000-0002-7745-3927

Wenqing Jiang − *Agricultural and Environmental Chemistry Graduate Group and Department of Environmental Toxicology, University of California, Davis, California 95616-5270, United States;* orcid.org/0000-0002-6869-3232

Cort Anastasio − *Department of Land, Air and Water Resources, University of California, Davis, California 95616-8627, United States; Agricultural and Environmental Chemistry Graduate Group, University of California, Davis, California 95616-5270, United States;* orcid.org/0000-0002-5373-0459

Qi Zhang − *Agricultural and Environmental Chemistry Graduate Group and Department of Environmental Toxicology, University of California, Davis, California 95616-5270, United States;* orcid.org/0000-0002-5203-8778

Alla Zelenyuk − *Pacific Northwest National Laboratory, Richland, Washington 99352, United States*

Complete contact information is available at: https://pubs.acs.org/10.1021/acs.est.3c07762

Notes

The authors declare no competing financial interest.

■ ACKNOWLEDGMENTS

This research is primarily supported by the U.S. Department of Energy (DOE) Office of Science Atmospheric System Research (ASR) project, by the DOE Office of Science Biological and Environmental Research (BER) Early Career Research Program at PNNL, and by the National Science Foundation (Grant 2220307) and the California Agricultural Experiment Station (projects CA-D-LAW-6403-RR and CA-D-ETX-2102-H). PNNL is operated for the Department of Energy by Battelle Memorial Institute under Contract DE-AC05-76 RL01830. Computational resources for the simulations were provided by EMSL (a DOE Office of Science User Facility sponsored by the Office of Biological and Environmental Research located at PNNL) and the PNNL Institutional Computing facility.

■ REFERENCES

(1) Tsimpidi, A. P.; Karydis, V. A.; Pandis, S. N.; Lelieveld, J. Global-scale combustion sources of organic aerosols: sensitivity to formation and removal mechanisms. *Atmospheric Chemistry and Physics* **2017**, *17* (12), 7345−7364.

(2) Tsimpidi, A. P.; Karydis, V. A.; Pandis, S. N.; Lelieveld, J. Global combustion sources of organic aerosols: model comparison with 84 AMS factor-analysis data sets. *Atmospheric Chemistry and Physics* **2016**, *16* (14), 8939−8962.

(3) Chen, J.; Li, C.; Ristovski, Z.; Milic, A.; Gu, Y.; Islam, M. S.; Wang, S.; Hao, J.; Zhang, H.; He, C.; et al. A review of biomass burning: Emissions and impacts on air quality, health and climate in China. *Sci. Total Environ.* **2017**, *579*, 1000−1034.

(4) Bikkina, S.; Andersson, A.; Kirillova, E. N.; Holmstrand, H.; Tiwari, S.; Srivastava, A. K.; Bisht, D. S.; Gustafsson, Ö. Air quality in megacity Delhi affected by countryside biomass burning. *Nature Sustainability* **2019**, *2* (3), 200−205.

(5) Zauscher, M. D.; Wang, Y.; Moore, M. J.; Gaston, C. J.; Prather, K. A. Air quality impact and physicochemical aging of biomass burning aerosols during the 2007 San Diego wildfires. *Environ. Sci. Technol.* **2013**, *47* (14), 7633−7643.

(6) Iinuma, Y.; Brüggemann, E.; Gnauk, T.; Müller, K.; Andreae, M.; Helas, G.; Parmar, R.; Herrmann, H. Source characterization of biomass burning particles: The combustion of selected European conifers, African hardwood, savanna grass, and German and Indonesian peat. *Journal of Geophysical Research: Atmospheres* **2007**, *112* (D8), D08209.

(7) Akagi, S.; Yokelson, R. J.; Wiedinmyer, C.; Alvarado, M.; Reid, J.; Karl, T.; Crounse, J.; Wennberg, P. Emission factors for open and domestic biomass burning for use in atmospheric models. *Atmospheric Chemistry and Physics* **2011**, *11* (9), 4039−4072.

(8) Yee, L.; Kautzman, K.; Loza, C.; Schilling, K.; Coggon, M.; Chhabra, P.; Chan, M.; Chan, A.; Hersey, S.; Crounse, J.; et al. Secondary organic aerosol formation from biomass burning intermediates: phenol and methoxyphenols. *Atmospheric Chemistry and Physics* **2013**, *13* (16), 8019−8043.

(9) Lim, C. Y.; Hagan, D. H.; Coggon, M. M.; Koss, A. R.; Sekimoto, K.; de Gouw, J.; Warneke, C.; Cappa, C. D.; Kroll, J. H. Secondary organic aerosol formation from the laboratory oxidation of biomass burning emissions. *Atmospheric Chemistry and Physics* **2019**, *19* (19), 12797−12809.
(10) Gilardoni, S.; Massoli, P.; Paglione, M.; Giulianelli, L.; Carbone, C.; Rinaldi, M.; Decesari, S.; Sandrini, S.; Costabile, F.; Gobbi, G. P.; et al. Direct observation of aqueous secondary organic aerosol from biomass-burning emissions. *Proc. Natl. Acad. Sci. U. S. A.* **2016**, *113* (36), 10013−10018.
(11) Shrivastava, M.; Cappa, C. D.; Fan, J.; Goldstein, A. H.; Guenther, A. B.; Jimenez, J. L.; Kuang, C.; Laskin, A.; Martin, S. T.; Ng, N. L.; et al. Recent advances in understanding secondary organic aerosol: Implications for global climate forcing. *Reviews of Geophysics* **2017**, *55* (2), 509−559.
(12) Cubison, M.; Ortega, A.; Hayes, P.; Farmer, D.; Day, D.; Lechner, M.; Brune, W.; Apel, E.; Diskin, G.; Fisher, J.; et al. Effects of aging on organic aerosol from open biomass burning smoke in aircraft and laboratory studies. *Atmospheric Chemistry and Physics* **2011**, *11* (23), 12049−12064.
(13) Meng, L.; Coeur, C.; Fayad, L.; Houzel, N.; Genevray, P.; Bouzidi, H.; Tomas, A.; Chen, W. Secondary organic aerosol formation from the gas-phase reaction of guaiacol (2-methoxyphenol) with NO3 radicals. *Atmos. Environ.* **2020**, *240*, 117740.
(14) Coeur-Tourneur, C.; Cassez, A.; Wenger, J. C. Rate coefficients for the gas-phase reaction of hydroxyl radicals with 2-methoxyphenol (guaiacol) and related compounds. *J. Phys. Chem. A* **2010**, *114* (43), 11645−11650.
(15) Nakao, S.; Clark, C.; Tang, P.; Sato, K.; Cocker, D., III Secondary organic aerosol formation from phenolic compounds in the absence of NO x. *Atmospheric Chemistry and Physics* **2011**, *11* (20), 10649−10660.
(16) Lauraguais, A.; Coeur-Tourneur, C.; Cassez, A.; Deboudt, K.; Fourmentin, M.; Choël, M. Atmospheric reactivity of hydroxyl radicals with guaiacol (2-methoxyphenol), a biomass burning emitted compound: Secondary organic aerosol formation and gas-phase oxidation products. *Atmospheric environment* **2014**, *86*, 155−163.
(17) Liu, C.; Liu, J.; Liu, Y.; Chen, T.; He, H. Secondary organic aerosol formation from the OH-initiated oxidation of guaiacol under different experimental conditions. *Atmos. Environ.* **2019**, *207*, 30−37.
(18) Li, F.; Tsona, N. T.; Li, J.; Du, L. Aqueous-phase oxidation of syringic acid emitted from biomass burning: Formation of light-absorbing compounds. *Science of The Total Environment* **2021**, *765*, 144239.
(19) Li, Y.; Huang, D.; Cheung, H. Y.; Lee, A.; Chan, C. K. Aqueous-phase photochemical oxidation and direct photolysis of vanillin-a model compound of methoxy phenols from biomass burning. *Atmospheric Chemistry and Physics* **2014**, *14* (6), 2871−2885.
(20) Misovich, M. V.; Hettiyadura, A. P. S.; Jiang, W.; Zhang, Q.; Laskin, A. Molecular-level study of the photo-oxidation of aqueous-phase guaiacyl acetone in the presence of 3c*: formation of brown carbon products. *ACS Earth and Space Chemistry* **2021**, *5* (8), 1983−1996.
(21) Lim, Y.; Tan, Y.; Perri, M.; Seitzinger, S.; Turpin, B. Aqueous chemistry and its role in secondary organic aerosol (SOA) formation. *Atmospheric Chemistry and Physics* **2010**, *10* (21), 10521−10539.
(22) Yu, L.; Smith, J.; Laskin, A.; Anastasio, C.; Laskin, J.; Zhang, Q. Chemical characterization of SOA formed from aqueous-phase reactions of phenols with the triplet excited state of carbonyl and hydroxyl radical. *Atmospheric Chemistry and Physics* **2014**, *14* (24), 13801−13816.
(23) Anastasio, C.; McGregor, K. G. Chemistry of fog waters in California's Central Valley: 1. In situ photoformation of hydroxyl radical and singlet molecular oxygen. *Atmos. Environ.* **2001**, *35* (6), 1079−1089.
(24) Badali, K.; Zhou, S.; Aljawhary, D.; Antiñolo, M.; Chen, W.; Lok, A.; Mungall, E.; Wong, J.; Zhao, R.; Abbatt, J. Formation of hydroxyl radicals from photolysis of secondary organic aerosol material. *Atmospheric Chemistry and Physics* **2015**, *15* (14), 7831−7840.
(25) Herrmann, H.; Hoffmann, D.; Schaefer, T.; Bräuer, P.; Tilgner, A. Tropospheric aqueous-phase free-radical chemistry: Radical sources, spectra, reaction kinetics and prediction tools. *ChemPhysChem* **2010**, *11* (18), 3796−3822.
(26) Tilgner, A.; Herrmann, H. Tropospheric aqueous-phase OH oxidation chemistry: Current understanding, uptake of highly oxidized organics and its effects. In *Multiphase environmental chemistry in the atmosphere*; American Chemical Society: 2018; pp 49−85.
(27) McNeill, K.; Canonica, S. Triplet state dissolved organic matter in aquatic photochemistry: reaction mechanisms, substrate scope, and photophysical properties. *Environmental Science: Processes & Impacts* **2016**, *18* (11), 1381−1399.
(28) Kaur, R.; Labins, J. R.; Helbock, S. S.; Jiang, W.; Bein, K. J.; Zhang, Q.; Anastasio, C. Photooxidants from brown carbon and other chromophores in illuminated particle extracts. *Atmospheric Chemistry and Physics* **2019**, *19* (9), 6579−6594.
(29) Smith, J. D.; Sio, V.; Yu, L.; Zhang, Q.; Anastasio, C. Secondary organic aerosol production from aqueous reactions of atmospheric phenols with an organic triplet excited state. *Environ. Sci. Technol.* **2014**, *48* (2), 1049−1057.
(30) Smith, J. D.; Kinney, H.; Anastasio, C. Phenolic carbonyls undergo rapid aqueous photodegradation to form low-volatility, light-absorbing products. *Atmos. Environ.* **2016**, *126*, 36−44.
(31) Smith, J. D.; Kinney, H.; Anastasio, C. Aqueous benzene-diols react with an organic triplet excited state and hydroxyl radical to form secondary organic aerosol. *Phys. Chem. Chem. Phys.* **2015**, *17* (15), 10227−10237.
(32) Jiang, W.; Misovich, M. V.; Hettiyadura, A. P.; Laskin, A.; McFall, A. S.; Anastasio, C.; Zhang, Q. Photosensitized reactions of a phenolic carbonyl from wood combustion in the aqueous phase—chemical evolution and light absorption properties of aqSOA. *Environ. Sci. Technol.* **2021**, *55* (8), 5199−5211.
(33) Arciva, S.; Niedek, C.; Mavis, C.; Yoon, M.; Sanchez, M. E.; Zhang, Q.; Anastasio, C. Aqueous· OH Oxidation of Highly Substituted Phenols as a Source of Secondary Organic Aerosol. *Environ. Sci. Technol.* **2022**, *56* (14), 9959−9967.
(34) Sun, Y.; Zhang, Q.; Anastasio, C.; Sun, J. Insights into secondary organic aerosol formed via aqueous-phase reactions of phenolic compounds based on high resolution mass spectrometry. *Atmospheric Chemistry and Physics* **2010**, *10* (10), 4809−4822.
(35) Xiao, Y.; Hu, M.; Li, X.; Zong, T.; Xu, N.; Hu, S.; Zeng, L.; Chen, S.; Song, Y.; Guo, S.; et al. Aqueous secondary organic aerosol formation attributed to phenols from biomass burning. *Science of The Total Environment* **2022**, *847*, 157582.
(36) McFall, A. S.; Johnson, A. W.; Anastasio, C. Air-water partitioning of biomass-burning phenols and the effects of temperature and salinity. *Environ. Sci. Technol.* **2020**, *54* (7), 3823−3830.
(37) Ma, L.; Guzman, C.; Niedek, C.; Tran, T.; Zhang, Q.; Anastasio, C. Kinetics and mass yields of aqueous secondary organic aerosol from highly substituted phenols reacting with a triplet excited state. *Environ. Sci. Technol.* **2021**, *55* (9), 5772−5781.
(38) Barzaghi, P.; Herrmann, H. Kinetics and mechanisms of reactions of the nitrate radical (NO3) with substituted phenols in aqueous solution. *Phys. Chem. Chem. Phys.* **2004**, *6* (23), 5379−5388.
(39) Ng, N. L.; Brown, S. S.; Archibald, A. T.; Atlas, E.; Cohen, R. C.; Crowley, J. N.; Day, D. A.; Donahue, N. M.; Fry, J. L.; Fuchs, H.; Griffin, R. J.; Guzman, M. I.; Herrmann, H.; Hodzic, A.; Iinuma, Y.; Jimenez, J. L.; Kiendler-Scharr, A.; Lee, B. H.; Luecken, D. J.; Mao, J.; McLaren, R.; Mutzel, A.; Osthoff, H. D.; Ouyang, B.; Picquet-Varrault, B.; Platt, U.; Pye, H. O. T.; Rudich, Y.; Schwantes, R. H.; Shiraiwa, M.; Stutz, J.; Thornton, J. A.; Tilgner, A.; Williams, B. J.; Zaveri, R. A. Nitrate radicals and biogenic volatile organic compounds: oxidation, mechanisms, and organic aerosol. *Atmos. Chem. Phys.* **2017**, *17* (3), 2103−2162.
(40) Feigenbrugel, V.; Le Calvé, S.; Mirabel, P.; Louis, F. Henry's law constant measurements for phenol, o-, m-, and p-cresol as a function of temperature. *Atmos. Environ.* **2004**, *38* (33), 5577−5588.

https://doi.org/10.1021/acs.est.3c07762
Environ. Sci. Technol. XXXX, XXX, XXX−XXX

(41) Sagebiel, J. C.; Seiber, J. N.; Woodrow, J. E. Comparison of headspace and gas-stripping methods for determining the Henry's law constant (H) for organic compounds of low to intermediate H. *Chemosphere* **1992**, *25* (12), 1763−1768.
(42) Sander, R. Compilation of Henry's law constants (version 5.0. 0) for water as solvent. *Atmospheric Chemistry and Physics* **2023**, *23* (19), 10901−12440.
(43) Tratnyek, P. G.; Hoigne, J. Oxidation of substituted phenols in the environment: a QSAR analysis of rate constants for reaction with singlet oxygen. *Environ. Sci. Technol.* **1991**, *25* (9), 1596−1604.
(44) Anastasio, C.; Faust, B. C.; Rao, C. J. Aromatic carbonyl compounds as aqueous-phase photochemical sources of hydrogen peroxide in acidic sulfate aerosols, fogs, and clouds. 1. Non-phenolic methoxybenzaldehydes and methoxyacetophenones with reductants (phenols). *Environ. Sci. Technol.* **1997**, *31* (1), 218−232.
(45) Ault, A. P. Aerosol acidity: Novel measurements and implications for atmospheric chemistry. *Acc. Chem. Res.* **2020**, *53* (9), 1703−1714.
(46) Craig, R. L.; Peterson, P. K.; Nandy, L.; Lei, Z.; Hossain, M. A.; Camarena, S.; Dodson, R. A.; Cook, R. D.; Dutcher, C. S.; Ault, A. P. Direct determination of aerosol pH: Size-resolved measurements of submicrometer and supermicrometer aqueous particles. *Analytical chemistry* **2018**, *90* (19), 11232−11239.
(47) Turnock, S.; Mann, G.; Woodhouse, M.; Dalvi, M.; O'Connor, F.; Carslaw, K.; Spracklen, D. The impact of changes in cloud water pH on aerosol radiative forcing. *Geophys. Res. Lett.* **2019**, *46* (7), 4039−4048.
(48) Scott, W. The pH of cloud water and the production of sulfate. *Atmospheric Environment (1967)* **1978**, *12* (4), 917−921.
(49) Woo, J.; McNeill, V. F. simpleGAMMA v1. 0-a reduced model of secondary organic aerosol formation in the aqueous aerosol phase (aaSOA). *Geoscientific Model Development* **2015**, *8* (6), 1821−1829.
(50) Budisulistiorini, S. H.; Nenes, A.; Carlton, A. G.; Surratt, J. D.; McNeill, V. F.; Pye, H. O. Simulating aqueous-phase isoprene-epoxydiol (IEPOX) secondary organic aerosol production during the 2013 Southern Oxidant and Aerosol Study (SOAS). *Environ. Sci. Technol.* **2017**, *51* (9), 5026−5034.
(51) Budisulistiorini, S.; Li, X.; Bairai, S.; Renfro, J.; Liu, Y.; Liu, Y.; McKinney, K.; Martin, S.; McNeill, V.; Pye, H.; et al. Examining the effects of anthropogenic emissions on isoprene-derived secondary organic aerosol formation during the 2013 Southern Oxidant and Aerosol Study (SOAS) at the Look Rock, Tennessee ground site. *Atmospheric Chemistry and Physics* **2015**, *15* (15), 8871−8888.
(52) Shrivastava, M.; Andreae, M. O.; Artaxo, P.; Barbosa, H. M.; Berg, L. K.; Brito, J.; Ching, J.; Easter, R. C.; Fan, J.; Fast, J. D.; et al. Urban pollution greatly enhances formation of natural aerosols over the Amazon rainforest. *Nat. Commun.* **2019**, *10* (1), 1046.
(53) McNeill, V. F. Aqueous organic chemistry in the atmosphere: Sources and chemical processing of organic aerosols. *Environ. Sci. Technol.* **2015**, *49*, 1237.
(54) Zhang, J.; Shrivastava, M.; Zelenyuk, A.; Zaveri, R. A.; Surratt, J. D.; Riva, M.; Bell, D.; Glasius, M. Observationally Constrained Modeling of the Reactive Uptake of Isoprene-Derived Epoxydiols under Elevated Relative Humidity and Varying Acidity of Seed Aerosol Conditions. *ACS Earth and Space Chemistry* **2023**, *7*, 788.
(55) Octaviani, M.; Shrivastava, M.; Zaveri, R. A.; Zelenyuk, A.; Zhang, Y.; Rasool, Q. Z.; Bell, D. M.; Riva, M.; Glasius, M.; Surratt, J. D. Modeling the Size Distribution and Chemical Composition of Secondary Organic Aerosols during the Reactive Uptake of Isoprene-Derived Epoxydiols under Low-Humidity Condition. *ACS Earth and Space Chemistry* **2021**, *5* (11), 3247−3257.
(56) Ervens, B.; Volkamer, R. Glyoxal processing by aerosol multiphase chemistry: towards a kinetic modeling framework of secondary organic aerosol formation in aqueous particles. *Atmospheric Chemistry and Physics* **2010**, *10* (17), 8219−8244.
(57) Knote, C.; Hodzic, A.; Jimenez, J.; Volkamer, R.; Orlando, J.; Baidar, S.; Brioude, J.; Fast, J.; Gentner, D.; Goldstein, A.; et al. Simulation of semi-explicit mechanisms of SOA formation from glyoxal in aerosol in a 3-D model. *Atmospheric Chemistry and Physics* **2014**, *14* (12), 6213−6239.
(58) Anttila, T.; Kiendler-Scharr, A.; Tillmann, R.; Mentel, T. F. On the reactive uptake of gaseous compounds by organic-coated aqueous aerosols: Theoretical analysis and application to the heterogeneous hydrolysis of N2O5. *J. Phys. Chem. A* **2006**, *110* (35), 10435−10443.
(59) Ge, X.; Setyan, A.; Sun, Y.; Zhang, Q. Primary and secondary organic aerosols in Fresno, California during wintertime: Results from high resolution aerosol mass spectrometry. *Journal of Geophysical Research-Atmospheres* **2012**, *117* (D19), D19301.
(60) Reyes-Villegas, E.; Priestley, M.; Ting, Y. C.; Haslett, S.; Bannan, T.; Le Breton, M.; Williams, P. I.; Bacak, A.; Flynn, M. J.; Coe, H.; Percival, C.; Allan, J. D. Simultaneous aerosol mass spectrometry and chemical ionisation mass spectrometry measurements during a biomass burning event in the UK: insights into nitrate chemistry. *Atmos. Chem. Phys.* **2018**, *18* (6), 4093−4111.
(61) Zhao, Z.; Wang, Q.; Li, L.; Han, Y.; Ye, Z.; Pongpiachan, S.; Zhang, Y.; Liu, S.; Tian, R.; Cao, J. Characteristics of PM2. 5 at a high-altitude remote site in the Southeastern margin of the Tibetan Plateau in premonsoon season. *Atmosphere* **2019**, *10* (11), 645.
(62) Fan, J.; Zhang, Y.; Li, Z.; Hu, J.; Rosenfeld, D. Urbanization-induced land and aerosol impacts on sea-breeze circulation and convective precipitation. *Atmospheric Chemistry and Physics* **2020**, *20* (22), 14163−14182.
(63) Friese, E.; Ebel, A. Temperature dependent thermodynamic model of the system H+- NH4+- Na+- SO42− NO3− Cl− H2O. *J. Phys. Chem. A* **2010**, *114* (43), 11595−11631.
(64) Zhang, D.; Li, Z.; Wu, H.; Wu, T.; Ren, R.; Cai, Z.; Liang, C.; Chen, L. Analysis of aerosol particle number size distribution and source attribution at three megacities in China. *Atmos. Environ.* **2022**, *279*, 119114.
(65) Young, D. E.; Kim, H.; Parworth, C.; Zhou, S.; Zhang, X.; Cappa, C. D.; Seco, R.; Kim, S.; Zhang, Q. Influences of emission sources and meteorology on aerosol chemistry in a polluted urban environment: results from DISCOVER-AQ California. *Atmospheric Chemistry and Physics* **2016**, *16* (8), 5427−5451.
(66) Li, H.; Zhang, Q.; Jiang, W.; Collier, S.; Sun, Y.; Zhang, Q.; He, K. Characteristics and sources of water-soluble organic aerosol in a heavily polluted environment in Northern China. *Science of The Total Environment* **2021**, *758*, 143970.
(67) Jiang, W.; Ma, L.; Niedek, C.; Anastasio, C.; Zhang, Q. Chemical and Light-Absorption Properties of Water-Soluble Organic Aerosols in Northern California and Photooxidant Production by Brown Carbon Components. *ACS Earth and Space Chemistry* **2023**, *7* (5), 1107−1119.
(68) Hoffmann, E. H.; Tilgner, A.; Wolke, R.; Böge, O.; Walter, A.; Herrmann, H. Oxidation of substituted aromatic hydrocarbons in the tropospheric aqueous phase: kinetic mechanism development and modelling. *Phys. Chem. Chem. Phys.* **2018**, *20* (16), 10960−10977.
(69) Surratt, J. D.; Chan, A. W.; Eddingsaas, N. C.; Chan, M.; Loza, C. L.; Kwan, A. J.; Hersey, S. P.; Flagan, R. C.; Wennberg, P. O.; Seinfeld, J. H. Reactive intermediates revealed in secondary organic aerosol formation from isoprene. *Proc. Natl. Acad. Sci. U. S. A.* **2010**, *107* (15), 6640−6645.
(70) Ying, Q.; Li, J.; Kota, S. H. Significant contributions of isoprene to summertime secondary organic aerosol in eastern United States. *Environ. Sci. Technol.* **2015**, *49* (13), 7834−7842.
(71) Fast, J. D.; Berg, L. K.; Alexander, L.; Bell, D.; D'Ambro, E.; Hubbe, J.; Kuang, C.; Liu, J.; Long, C.; Matthews, A.; et al. Overview of the HI-SCALE field campaign: A new perspective on shallow convective clouds. *Bulletin of the American Meteorological Society* **2019**, *100* (5), 821−840.
(72) Shrivastava, M.; Rasool, Q. Z.; Zhao, B.; Octaviani, M.; Zaveri, R. A.; Zelenyuk, A.; Gaudet, B.; Liu, Y.; Shilling, J. E.; Schneider, J.; et al. Tight Coupling of Surface and In-Plant Biochemistry and Convection Governs Key Fine Particulate Components over the Amazon Rainforest. *ACS Earth and Space Chemistry* **2022**, *6* (2), 380−390.

https://doi.org/10.1021/acs.est.3c07762
Environ. Sci. Technol. XXXX, XXX, XXX−XXX

(73) Schulz, C.; Schneider, J.; Amorim Holanda, B.; Appel, O.; Costa, A.; de Sá, S. S.; Dreiling, V.; Fütterer, D.; Jurkat-Witschas, T.; Klimach, T.; et al. Aircraft-based observations of isoprene-epoxydiol-derived secondary organic aerosol (IEPOX-SOA) in the tropical upper troposphere over the Amazon region. *Atmospheric chemistry and physics* **2018**, *18* (20), 14979−15001.
(74) Tsui, W. G.; Woo, J. L.; McNeill, V. F. Impact of aerosol-cloud cycling on aqueous secondary organic aerosol formation. *Atmosphere* **2019**, *10* (11), 666.
(75) Otto, T.; Schaefer, T.; Herrmann, H. Aqueous-phase oxidation of cis-*β*-isoprene epoxydiol by hydroxyl radicals and its impact on atmospheric isoprene processing. *J. Phys. Chem. A* **2019**, *123* (49), 10599−10608.
(76) Ma, L.; Worland, R.; Jiang, W.; Niedek, C.; Guzman, C.; Bein, K. J.; Zhang, Q.; Anastasio, C. Predicting photooxidant concentrations in aerosol liquid water based on laboratory extracts of ambient particles. *Atmospheric Chemistry and Physics* **2023**, *23* (23), 8805−8821.

https://doi.org/10.1021/acs.est.3c07762
Environ. Sci. Technol. XXXX, XXX, XXX−XXX